

## Optical trapping and manipulation of magnetic holes dispersed in a magnetic fluid

Ting Sun,<sup>1</sup> Zhi-Cheng Fu,<sup>1</sup> Wei-Ren Zhao,<sup>2</sup> Hai-Dong Deng,<sup>1</sup> Qiao-Feng Dai,<sup>1</sup> Li-Jun Wu,<sup>1</sup> Sheng Lan,<sup>1,a)</sup> and Achanta Venu Gopal<sup>3</sup>

<sup>1</sup>Laboratory of Photonic Information Technology, School for Information and Optoelectronic Science and Engineering, South China Normal University, Guangzhou, Guangdong 510006, People's Republic of China

<sup>2</sup>School of Physics and Optoelectronics, Guangdong University of Technology, Guangzhou, Guangdong 510006, People's Republic of China

<sup>3</sup>Department of Condensed Matter Physics and Material Science, Tata Institute of Fundamental Research, Homi Bhabha Road, Mumbai 400005, India

(Received 12 November 2009; accepted 11 March 2010; published online 6 May 2010)

The optical trapping and manipulation of magnetic holes (MHs) dispersed in a magnetic fluid is systematically investigated. It is found that the gradient force, which tends to attract MHs to the beam center, can be completely counteracted by the repulsive force between MHs induced by a magnetic field. As a result, a depletion region is created at the laser beam spot for a sufficiently strong magnetic field. This phenomenon can be easily observed for large MHs with a diameter of 11  $\mu\text{m}$ . However, it does not appear for MHs with a smaller diameter of 4.3  $\mu\text{m}$ . It is revealed that the enhancement in the concentration of magnetic nanoparticles in the laser spot region as well as the clustering of these nanoparticles leads to a much stronger interaction between MHs when a magnetic field is applied. Consequently, the magnetic field strength necessary to create the depletion region is significantly reduced. We also find that the trapping behavior of MHs depends strongly on the thickness of the sample cells. For thin sample cells in which only one layer (or a two-dimensional distribution) of MHs is allowed, we can observe the creation of depletion region. In sharp contrast, MHs can be stably trapped at the center of the laser beam in thick sample cells even if a strong magnetic field is imposed. This phenomenon can be explained by the existence of a gradient in magnetic field strength along the direction perpendicular to the sample cells. Apart from individual MHs, we also investigate the movement of MH chains under the scattering force of the laser beam. It is observed that MH chains always move along the direction parallel to the magnetic field. This behavior can be easily understood when the anisotropy in viscosity caused by the applied magnetic field is considered. © 2010 American Institute of Physics.

[doi:[10.1063/1.3386522](https://doi.org/10.1063/1.3386522)]

### I. INTRODUCTION

Since the pioneering work of Ashkin,<sup>1,2</sup> optical trapping and manipulation of objects in micro- and nanometer scales have attracted great interest in the last two decades because of their potential applications in various fields of science and technology.<sup>3</sup> In most cases, micro- or nanoparticles to be manipulated are usually dispersed into a carrier liquid such as water. As a result, the weight of these particles is partially or completely balanced by the floating force supplied by the liquid, making the optical trapping and manipulation more convenient. In early experiments, an aqueous solution of micrometer-sized polystyrene (PS) spheres was generally used as a platform to study the trapping of individual and multiple particles.<sup>1,2</sup>

Magnetic fluids or ferrofluids are a kind of colloidal liquids in which magnetic nanoparticles are uniformly distributed in a carrier liquid such as water or kerosene.<sup>4</sup> They have also received intensive studies in the last two decades because the formation of magnetic chains or columns in the

presence of an external magnetic field gives rise to many interesting phenomena such as birefringence,<sup>5-7</sup> modulation of optical transmission,<sup>8-10</sup> and magnetochromatics<sup>11,12</sup> etc. It is expected that these phenomena can be employed to realize some important magneto-optical devices such as optical switches,<sup>9,13,14</sup> tunable gratings,<sup>15-17</sup> and magnetic field sensors<sup>18,19</sup> etc. Early in 1983, the physical properties of PS spheres immersed into a magnetic fluid were investigated by Skjeltorp.<sup>20</sup> It was found that each PS sphere can acquire a magnetic moment due to the magnetization of the surrounding magnetic fluid.<sup>20,21</sup> Consequently, a regular arrangement of PS spheres was realized through the repulsive and attractive interaction between the induced magnetic moments.<sup>20,22,23</sup> It means that the arrangement of nonmagnetic particles can be controlled by a magnetic field through a magnetic fluid. Nowadays, such nonmagnetic objects are generally referred to as magnetic holes (MHs). It seems quite interesting to study the optical trapping and manipulation of MHs because of the following reasons. First, the simultaneous control or manipulation of MHs with the combination of an optical and a magnetic field has not been investigated. Thus, lot of useful information concerning the optical forces

<sup>a)</sup>Author to whom correspondence should be addressed. Electronic mail: slan@scnu.edu.cn.

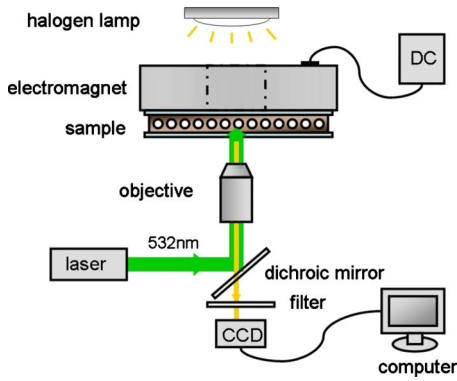


FIG. 1. (Color online) Schematic of the experimental setup used to investigate the optical trapping and manipulation of MHs.

and interaction energy of MHs can be extracted. Second, the physical properties of the magnetic fluid such as refractive index and viscosity can be easily modified by applying a magnetic field. This modification may affect the trapping behavior of MHs. Finally, the trapping behavior of MHs may be significantly modified because laser light has been employed to induce the diffusion and clustering of magnetic nanoparticles.

In this article, we present a systematic investigation of the optical trapping and manipulation of MHs. It is organized as follows. In Sec. II, the preparation of the samples and the experimental setup are described. Then, the optical and repulsive forces acting on MHs are analyzed in Sec. III. After that, the optical trapping of large and small MHs in thin and thick samples are compared and discussed in Secs. IV–VI. In addition, the optical manipulation of MH chains is presented in Sec. VII. Finally, a summary of our research work is given in the conclusion.

## II. SAMPLE PREPARATION AND EXPERIMENTAL SETUP

In order to investigate the optical trapping of MHs under different conditions, we have prepared samples containing MHs of different diameters (11 and 4.3  $\mu\text{m}$ ). They were obtained by uniformly dispersing PS spheres into a magnetic fluid. The magnetic fluid used in our study was the water-based  $\text{Fe}_3\text{O}_4$  fabricated by the chemical coprecipitation technique. The average diameter of magnetic nanoparticles is  $\sim 12$  nm and their volume fraction in the magnetic fluid is 7.9%. In experiments, we mixed the aqueous solution of PS spheres with a concentration of 10% (Duck Corp.) and the magnetic fluid with a mixing ratio of 3:1. The PS spheres were uniformly dispersed into the magnetic fluid by sonication, forming MHs. The purpose of choosing MHs with different diameters is to find out the size dependence of optical trapping behavior. Apart from sample cells containing different MHs, sample cells with different thicknesses (20 and 50  $\mu\text{m}$ ) were also used in the experiments and they are denoted as thin and thick sample cells, respectively.

The experimental setup used in our study is schematically shown in Fig. 1. The 532-nm light from a solid-state laser (Coherent Verdi-5) was introduced into an inverted microscope (Zeiss Axio Observer A1) and focused into the

sample cells by using a  $63\times$  objective lens. A charge coupled device connected to the microscope was employed to monitor the distribution and movement of MHs induced by the optical forces of the focused laser beam with or without the application of a magnetic field. The magnetic field applied perpendicularly or parallel to the sample cells was supplied by a solenoid which was placed just on top of the sample cells. The strength of the magnetic field was changed by adjusting the current of the solenoid.

## III. OPTICAL AND REPULSIVE FORCES ACTING ON MHS

Since the wavelength of the trapping light (0.532  $\mu\text{m}$ ) is much smaller than the diameters of the MHs used in this study (11 or 4.3  $\mu\text{m}$ ), the optical forces acting on MHs can be analyzed and calculated based on ray optics. In this case, the optical forces depend strongly on the location of the MHs with respect to the laser beam. The accurate calculation of the optical forces is complicated and a detailed analysis can be found in Ref. 24. In this article, our main purpose is not the calculation of these optical forces. Therefore, it is sufficient to qualitatively understand the optical forces exerted on MHs which include the gradient force in the transverse and longitudinal directions and the scattering force in the forward direction.

As compared with the optical forces, the repulsive force and the corresponding interaction energy between MHs induced by a magnetic field can be easily estimated. Under a magnetic field, each PS sphere surrounded by magnetic fluid acquires a magnetic moment that can be described as follows<sup>20,23</sup>

$$\mathbf{m}_i = -4\pi r^3 \frac{\chi_f}{2\chi_f + 3} \mathbf{H}_{ext}. \quad (1)$$

Here,  $r$  is the radius of MHs,  $\chi_f$  is the magnetic susceptibility of the magnetic fluid, and  $\mathbf{H}_{ext}$  is the strength of the external magnetic field. Thus, the interaction energy between two MHs can be expressed as<sup>20,21</sup>

$$U_i = \frac{\mu_0(1 + \chi_f)}{4\pi} \mathbf{m}_i^2 \left( \frac{1 - 3 \cos^2 \theta}{a^3} \right), \quad (2)$$

where  $\mu_0 = 4\pi \times 10^{-7} \text{ Hm}^{-1}$  is the magnetic permeability of free space,  $\theta$  is the angle between the magnetic field direction and the sample cell, and  $a$  is the distance between the two MHs.

When a magnetic field normal to the sample cell is applied, the interaction energy reaches its maximum value when the two MHs contact with each other. The maximum interaction energy is given by

$$U_{ir \max} = -\frac{\mu_0(1 + \chi_f)}{2\pi a^3} \mathbf{m}_i^2. \quad (3)$$

For 11- $\mu\text{m}$  and 4.3- $\mu\text{m}$  MHs, the maximum interaction energy is achieved when  $a = 11 \mu\text{m}$  and  $a = 4.3 \mu\text{m}$ , respectively. It is found that the maximum interaction energy for 11- $\mu\text{m}$  MHs is about 16.7 times of that for 4.3- $\mu\text{m}$  MHs. However, the gradient force in the transverse direction is estimated to be similar for these two types of MHs.<sup>24,25</sup> It

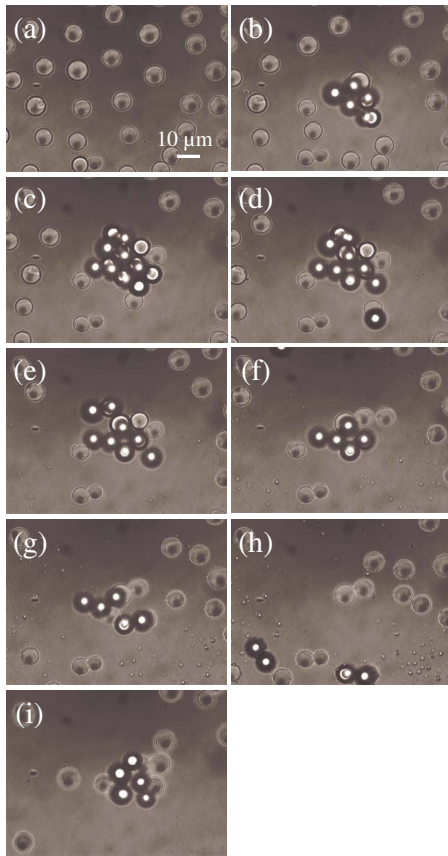


FIG. 2. (Color online) Optical trapping of 11- $\mu\text{m}$  MHs contained in a thin sample cell. (a) The initial distribution of MHs; (b) The trapping light with a power of 50 mW was turned on; [(c)–(h)]. A magnetic field of 40, 80, 100, 120, 140, and 160 Oe was imposed perpendicularly on the sample cell. (i) The magnetic field was removed.

means that the optical potential wells for them have similar depths. This feature implies that the trapping behavior could be much different for these two types of MHs.

#### IV. OPTICAL TRAPPING OF LARGE MHS IN A THIN SAMPLE CELL

Let us first examine the trapping behavior of 11- $\mu\text{m}$  MHs sealed in a thin sample cell of 20  $\mu\text{m}$ . The initial distribution of MHs is presented in Fig. 2(a). Once a laser beam with a power of 50 mW was focused into the sample cell, the MHs within the beam region were quickly driven to the beam center by the gradient force in the transverse direction, as shown in Fig. 2(b). Since the scattering force was larger than the gradient force in the longitudinal direction, MHs were pushed to the top wall of the sample cell and trapped there. They appear as bright spots surrounded by dark rings. Under this condition, a magnetic field was imposed perpendicularly on the sample and its strength was gradually increased. Due to magnetization by the applied magnetic field, magnetic nanoparticles uniformly dispersed in the magnetic field began to aggregate into clusters with increasing magnetic field. Meanwhile, each MH acquires a magnetic moment that is anti-parallel to the magnetic field.<sup>20</sup> The formation of magnetic clusters leads to an increase in the refractive index of the magnetic fluid, weakening the gradient force acting on MHs. However, it was found that the refractive

index of a 80- $\mu\text{m}$  magnetic fluid film was increased only slightly from 1.435 to 1.445 for light at 1.557  $\mu\text{m}$ .<sup>26</sup> In our case, we have employed a technique based on Fresnel reflection<sup>27</sup> to measure the refractive index of the magnetic fluid at 1.55  $\mu\text{m}$  and found a slight increase in refractive index from 1.3347 to 1.3362. Thus, it is expected that the variation in refractive index is also small at 532 nm although the measurement of refractive index is not easy at this wavelength due to the large absorption of magnetic nanoparticles. Therefore, we think that the slight increase in refractive index does not affect too much the gradient force acting on MHs.

Apart from the gradient force, the induced magnetic moments in MHs results in a repulsive interaction between them. When the magnetic field was weak, however, the MHs remain trapped at the beam center. In addition, MHs that occasionally diffused into the beam region were also captured to the beam center, as shown in Figs. 2(c). However, the situation changed when the magnetic field was increased to  $\sim 80$  Oe. As can be seen in Fig. 2(d), the strong attraction between MHs was released due mainly to the strong repulsive force between them. The repulsive interaction between MHs increased their energy and some MHs began to escape from the optical trap once the interaction energy became comparable to the depth of the optical potential well. As shown in Figs. 2(e)–2(g), more and more MHs escaped out of the optical trap and diffused away. Under a magnetic field of  $\sim 160$  Oe, no MH was found in the beam region [see Fig. 2(h)]. Sometimes, only one MH was left in the optical trap. If we switched-off the magnetic field, MHs that diffused into the beam region could again be trapped, as shown in Fig. 2(i). This phenomenon indicates that the gradient force exerted on MHs can be completely counteracted by the repulsive force induced by the magnetic field.

So far, we have demonstrated the optical trapping of randomly distributed MHs and the escape of these MHs from the optical potential well caused by an applied magnetic field. Now let us see what will happen when a laser beam with the same power (50 mW) is incident on MHs which have been organized into a two-dimensional (2D) regular lattice under a magnetic field. In experiments, we used the same sample described above. A magnetic field of  $\sim 100$  Oe was applied perpendicularly on the sample. As shown in Fig. 3(a), MHs were self-organized into a 2D hexagonal lattice due to the repulsive interaction between them. Under this condition, we turned on the trapping light. Surprisingly, MHs did not move to the beam center. Instead, they were driven out of the optical potential well, leaving a depletion region at the beam center [see Fig. 3(b)]. This depletion region became larger after some time, as shown in Figs. 3(c) and 3(d). In this case, it is thought that the concentration of magnetic nanoparticles were increased by both the optical trapping effect and the thermal diffusion of nanoparticles. In addition, clustering of magnetic nanoparticles also occurs because of laser irradiation. These phenomena have been reported in earlier work<sup>13</sup> and they are expected to enhance the induced magnetic moments in MHs. The clustering of magnetic nanoparticles under the irradiation of a light was first reported by Hoffmann *et al.*<sup>28</sup> Two years ago, we observed that

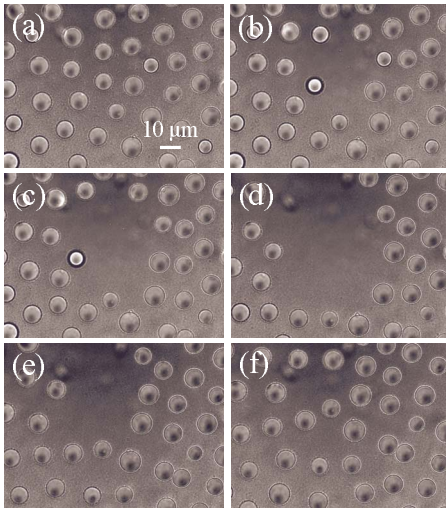


FIG. 3. (Color online) Optical trapping of 11- $\mu\text{m}$  MHs contained in a thin sample cell in the presence of a magnetic field. (a) The initial distribution of MHs in the presence of a magnetic field of 100 Oe; [(b)–(d)]. The distribution of MHs 10, 20, and 40 s after a trapping light of 50 mW was turned on. [(e)–(f)]. The distribution of MHs 30 and 90 s after the trapping light was turned-off.

large magnetic clusters appeared first in the region irradiated by a laser beam once a magnetic field was imposed.<sup>13</sup> It was suggested that small magnetic clusters, which acted as nuclei for the formation of large magnetic clusters, had been created under the irradiation of the laser beam. Very recently, we presented further evidence for the formation of magnetic clusters induced by a laser beam.<sup>29</sup> The formation a photonic gap was clearly observed in a magnetic fluid when a laser light or a magnetic field is imposed. In addition, the center of the photonic gap shifts to longer wavelength with increasing laser power. It is thought that both optical trapping and thermal diffusion of magnetic nanoparticles are responsible for the appearance of magnetic clusters.

According to Eq. (2), a significant increase in the interaction energy is anticipated. Consequently, the repulsive force existing between MHs may become much larger than the gradient force even at a moderate magnetic field of  $\sim 100$  Oe. Therefore, MHs could not be trapped by the optical potential well. Instead, they were driven away from the beam center. If we turned-off the trapping light, the depletion region shrank after 30 s and completely disappeared after about 90 s, as shown in Figs. 3(e) and 3(f).

In order to verify that the formation of the depletion region was caused by the increase in the concentration of magnetic nanoparticles, we carried out another experiment to characterize the repulsive interaction of close-packed MHs in the absence of laser irradiation. It is shown in Fig. 4. First, a 50 mW laser beam was employed to trap some MHs at the beam center. Then, the trapping light was turned off while a magnetic field of  $\sim 100$  Oe was imposed perpendicularly on the sample. In this case, the repulsive force between MHs was not significant and they were not separated immediately. The MHs being trapped remained at the beam center for several seconds. After about 40 s, the MHs diffused away due to Brownian motion. This situation is shown in Fig. 4. Therefore, a depletion region cannot be created if a magnetic

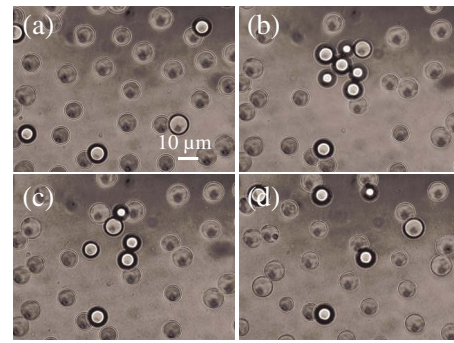


FIG. 4. (Color online) Repulsive interaction between 11- $\mu\text{m}$  MHs induced by an applied magnetic field. (a) The initial distribution of MHs. (b) Trapping of MHs at the beam center by a 50 mW laser light; [(c)–(d)]. Distribution of MHs 5 and 40 s after the trapping light was withdrawn while a 100 Oe magnetic field was imposed.

field is applied after the withdrawn of the trapping light. Of course, the original regular distribution of MHs was recovered after some time (not shown), similar to that shown in Fig. 3(f).

#### V. DEPENDENCE OF TRAPPING BEHAVIOR ON THE SIZE OF MHs

From Eqs. (1) and (2) described in Sec. III, it can be easily derived that the interaction energy between two identical MHs is proportional to the square of their volume. In order to find out the influence of the size of MHs on the repulsive interaction between them, we have performed similar experiments for 4.3- $\mu\text{m}$  MHs contained in a thin sample cell. As indicated in Sec. III, the maximum interaction energy for 4.3- $\mu\text{m}$  MHs is reduced by a factor of  $\sim 16.7$  as compared to that for 11- $\mu\text{m}$  ones. Therefore, it is not easy for 4.3- $\mu\text{m}$  MHs to escape out of the optical trap if the same trapping conditions are employed.

The images showing the trapping of 4.3- $\mu\text{m}$  MHs with increasing magnetic field are presented in Fig. 5. Similarly, the power of the trapping light was fixed at 50 mW and it was kept on during the increase of the magnetic field. The maximum magnetic field used in this case was increased to 400 Oe and the total trapping time was estimated to be 400 s when the magnetic field was raised to this value. Different from 11- $\mu\text{m}$  MHs, it is found that 4.3- $\mu\text{m}$  MHs were stably trapped at the beam center till a magnetic field as large as 400 Oe. With increasing magnetic field, more and more MHs were trapped at the beam center, forming a close-packed structure whose size is much larger than the focus. It is noticed that MHs were also trapped at the top wall of the sample cell due to the scattering force.

Similar to the above experiment carried out for 11- $\mu\text{m}$  MHs (see Fig. 3), we also tried to identify the repulsive interaction between 4.3- $\mu\text{m}$  MHs by applying a magnetic field on the sample before turning on the trapping light. Since there is significant reduction in repulsive interaction, no regular distribution was obtained after the application of a magnetic field of  $\sim 100$  Oe, as shown in Fig. 6(a). When the trapping light was introduced, however, no depletion region was observed. On the contrary, MHs were gradually attracted to the beam center after some time and the number of

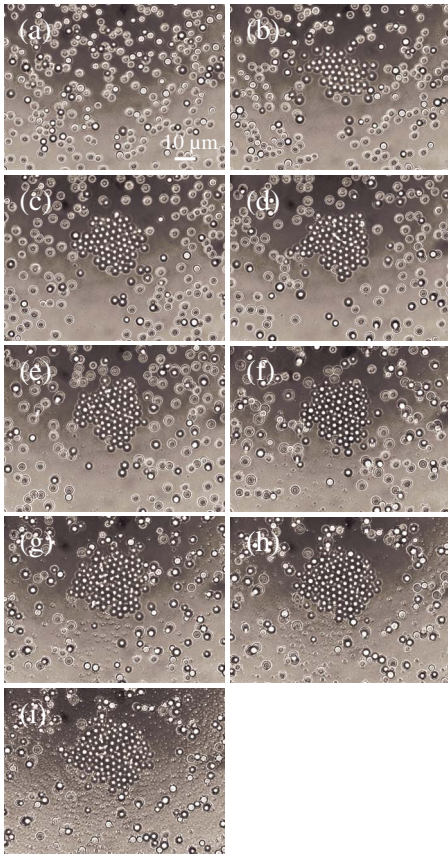


FIG. 5. (Color online) Optical trapping of 4.3- $\mu\text{m}$  MHs contained in a thin sample cell. (a) The initial distribution of MHs. (b) The trapping light with a power of 50 mW was turned on; [(c)–(i)]. A magnetic field of 40, 80, 120, 160, 200, 240, and 400 Oe was imposed perpendicularly on the sample cell.

trapped MHs increased with time, as shown in Figs. 6(b) and 6(c). After about 40 s, several tens of MHs were trapped in the beam region. On the other hand, the MHs being trapped did not form a close-packed structure as that shown in Fig. 5 because of the shorter trapping time. They were separated with each other by a distance due to the enhanced repulsive interaction between them.

## VI. OPTICAL TRAPPING OF LARGE MHS IN A THICK SAMPLE CELL

It has been shown that 11- $\mu\text{m}$  MHs cannot be stably trapped in a thin sample cell if the applied magnetic field is

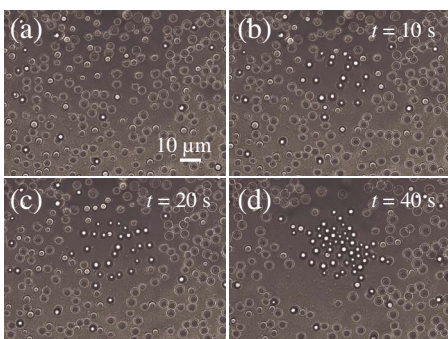


FIG. 6. (Color online) Optical trapping of 4.3- $\mu\text{m}$  MHs contained in a thin sample cell in the presence of a magnetic field. (a) The initial distribution of MHs in the presence of a magnetic field of 100 Oe; [(b)–(c)]. The distribution of MHs 10, 20, and 40 s after a trapping light of 50 mW was turned on.

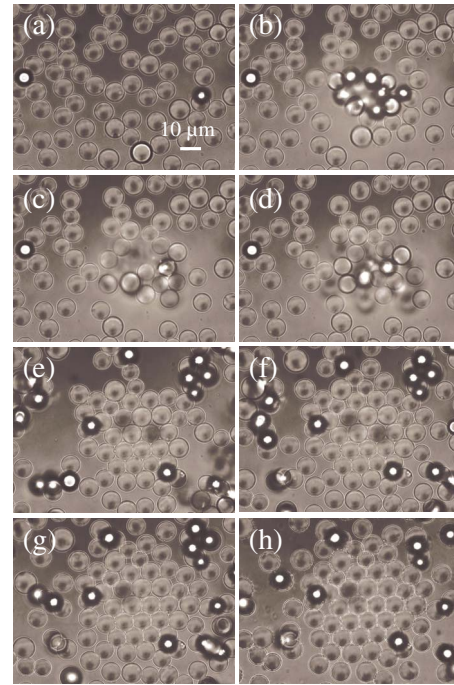


FIG. 7. (Color online) Optical trapping of 11- $\mu\text{m}$  MHs contained in a thick sample cell. (a) The initial distribution of MHs; [(b)–(d)]. The trapping light with a power of 50 mW was turned on; [(e)–(h)]. A magnetic field of 40, 80, 120, and 160 Oe was imposed perpendicularly on the sample cell.

strong enough. The interaction energy between MHs can easily exceed the optical potential, leading to the escape of MHs. However, we found that the trapping behavior could be dramatically changed when a thick sample cell of 50  $\mu\text{m}$  was used.

As mentioned above, MHs are trapped at the top wall of the thin sample cell because the thickness of the sample cell is slightly larger than the diameter of 11- $\mu\text{m}$  MHs. For a thick sample cell of 50- $\mu\text{m}$ , the situation is completely different. It was observed that MHs were driven quickly to the top wall of the sample cell and scattered away from the beam region, as shown in Figs. 7(b)–7(d). When a magnetic field of  $\sim 40$  Oe was imposed, it was found that some MHs began to be trapped at the bottom wall of the sample cell and the number of trapped MHs increased with increasing magnetic field, as shown in Figs. 7(e)–7(h). These MHs appear as dark and big circles in the images. It is also noticed that these MHs formed a close-packed structure. This behavior is completely different from what we observed in the thin sample cell. It implies that the repulsive interaction between MHs was significantly reduced and the gradient force became dominant again in the transverse direction.

It is well known that magnetic nanoparticles absorb visible light, leading to the heating of the magnetic fluid. In this case, thermal gradients may be established in both the horizontal and vertical directions. In the horizontal (transverse) direction, the thermal gradient leads to the redistribution of magnetic nanoparticles. This phenomenon, which is generally referred to as Soret effect, may significantly affect the trapping behavior of MHs. A typical example has been shown in Fig. 3. On the other hand, the thermal gradient in vertical direction may cause Rayleigh–Benard convection if

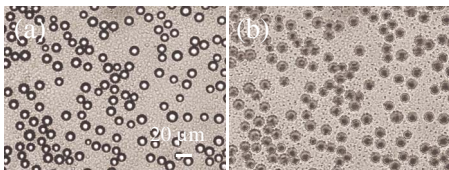


FIG. 8. (Color online) Distribution of 11- $\mu\text{m}$  MHs and magnetic clusters in a thick sample cell under a magnetic field of 100 Oe. The focus point of the objective lens was located at (a) the bottom and (b) the top walls of the sample cell.

the Rayleigh number becomes larger than 1708.<sup>30</sup> In order to find out the physical origin for the fast moving of MHs in the thick sample cell, we have employed the 800-nm light from a femtosecond laser (Coherent, Mira 900) as the trapping light. The absorption of magnetic nanoparticles is very weak at this wavelength.<sup>28</sup> It was observed that MHs remained nearly unmoved or moved very slowly under the irradiation of the 800-nm light with a power of 100 mW. It indicates that the scattering force is not responsible for the fast moving of MHs observed in the thick sample cell. Instead, it is suggested that Rayleigh–Benard convection occurred in the thick sample cell because the Rayleigh number increases at the third power of the sample thickness.

In order to find out the physical mechanism responsible for the strange trapping behavior observed in the thick sample cell, we have carefully examined the formation of magnetic clusters as well as the distribution of MHs near the bottom and top walls of the sample cell in the presence of a magnetic field, as shown in Figs. 8(a) and 8(b). From Fig. 8(a) where the objective lens was focused at the bottom of the sample cell, it can be seen that all MHs are distributed at the bottom wall of the sample cell. No MH is found to locate in the middle of the sample cell. Otherwise, we should be able to see some MHs which are out of focus. When we moved the focus point to the top wall, it was observed that all MHs became out of focus. In this case, one can clearly identify many magnetic clusters formed by the aggregation of magnetic nanoparticles, as shown in Fig. 8(b). These magnetic clusters appear as bright spots in Fig. 8(a) where they are out of focus.

The formation of magnetic clusters near the top wall of the sample cell implies a larger concentration of magnetic nanoparticles as compared to that near the bottom wall. In other words, there exists a gradient in the concentration of magnetic nanoparticles when a magnetic field was applied. It may be caused by the gradient in magnetic field strength. For the thin sample cell, the effect of such a gradient can be neglected. However, it becomes significant for the thick sample cell. Driven by the gradient in magnetic field, a depletion of magnetic nanoparticles occurs at the bottom part of the sample cell while an accumulation of magnetic nanoparticles appears at the top part of the sample cell. Meanwhile, MHs were driven to the bottom of the sample cell. Due to the depletion of magnetic nanoparticles at the bottom part of the sample cell, the repulsive force between MHs was significantly reduced. As a result, they were stably trapped at the beam center, forming a close-packed structure. Besides, the upward driving force originating from the convection of

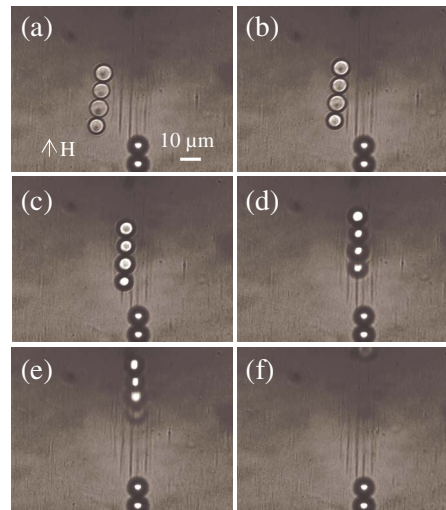


FIG. 9. (Color online) Trapping, scattering, and escaping processes of MH chains in the presence of a parallel magnetic field.

the magnetic fluid was counteracted by the downward driving force induced by the redistribution of magnetic nanoparticles. Consequently, MHs were pressed to the bottom wall of the sample cell.

## VII. OPTICAL MANIPULATION OF MH CHAINS

So far, we have investigated the trapping of individual MHs under a magnetic field perpendicular to the sample cells. The situation is completely different if we applied a magnetic field parallel to the thick sample cell containing 11- $\mu\text{m}$  MHs. In this case, MH chains were formed due to the attractive interaction between MHs.<sup>20</sup> When the trapping light was turned on, the gradient force in the transverse direction drove the MH chain that diffused into the beam region toward the beam center. Then, the MH chain was pushed to the top wall of the sample cell by both the convection of the magnetic fluid and the scattering force. Finally, it moved away from the beam region along the direction of the applied magnetic field. A typical example is presented in Fig. 9 which shows the trapping, scattering and escaping processes of a MH chain. An intriguing feature for the optical manipulation of MH chains is the movement of MH chains which always follows the direction of the magnetic field.

It has been reported that the viscosity of a magnetic fluid becomes anisotropic upon the application of a magnetic field.<sup>31</sup> Due to the formation of magnetic clusters and chains, the viscosity in the direction perpendicular to the magnetic field can be much larger than that in the direction parallel to the magnetic field. In Fig. 9, one can identify many magnetic chains aligned along the magnetic field. The anisotropy in the viscosity leads to the directional movement of MH chains. This character offers us an opportunity to optically drive MH chains along a selected direction with the help of a magnetic field.

## VIII. CONCLUSION

The optical trapping and manipulation of MHs have been systematically investigated. The trapping behavior is found to depend strongly on the size of MHs as well as the thickness of the sample cells. In thin sample cells of 20  $\mu\text{m}$ , a stable optical trapping under a magnetic field is available only for small MHs with a diameter of 4.3  $\mu\text{m}$ . For large MHs with a diameter of 11- $\mu\text{m}$ , a depletion region is created at the beam center for a sufficiently strong magnetic field because the gradient force is completely counteracted by the repulsive force induced by the magnetic field. In thick sample cells of 50  $\mu\text{m}$ , a stable optical trapping for 11- $\mu\text{m}$  MHs becomes possible because of the existence of a gradient in the magnetic field. It is also revealed that the movement of MH chains can be manipulated under a parallel magnetic field. Our findings may be useful for the construction of magneto-optical devices based on MHs.

## ACKNOWLEDGMENTS

The authors acknowledge the financial support from the National Natural Science Foundation of China (Grant Nos. 10974060 and 10774050) and the Program for Innovative Research Team of the Higher Education in Guangdong province of China (Grant No. 06CXTD005).

<sup>1</sup>A. Ashkin, *Phys. Rev. Lett.* **24**, 156 (1970).

<sup>2</sup>A. Ashkin, J. M. Dziedzic, J. E. Bjorkholm, and S. Chu, *Opt. Lett.* **11**, 288 (1986).

<sup>3</sup>A. Ashkin, *Proc. Natl. Acad. Sci. U.S.A.* **94**, 4853 (1997).

<sup>4</sup>R. E. Rosensweig, *Sci. Am.* **247**, 136 (1982).

<sup>5</sup>M. Xu and P. J. Ridler, *J. Appl. Phys.* **82**, 326 (1997).

<sup>6</sup>N. A. Yusuf, H. A. Safia, and I. A. Aljarayesh, *J. Appl. Phys.* **73**, 6136 (1993).

<sup>7</sup>Z. Y. Di, X. F. Chen, S. L. Pu, X. Hu, and Y. X. Xia, *Appl. Phys. Lett.* **89**,

211106 (2006).

<sup>8</sup>S. Y. Yang, Y. P. Chiu, B. Y. Jeang, and H. E. Horng, *Appl. Phys. Lett.* **79**, 2372 (2001).

<sup>9</sup>H. E. Horng, C. S. Chen, K. L. Fang, S. Y. Yang, and J. J. Chieh, *Appl. Phys. Lett.* **85**, 5592 (2004).

<sup>10</sup>J. E. Martin, K. M. Hill, and C. P. Tigges, *Phys. Rev. E* **59**, 5676 (1999).

<sup>11</sup>H. E. Horng, C. Y. Hong, W. B. Yeung, and H. C. Yang, *Appl. Opt.* **37**, 2674 (1998).

<sup>12</sup>S. Y. Yang, J. J. Chieh, H. E. Horng, C. Y. Hong, and H. C. Yang, *Appl. Phys. Lett.* **84**, 5204 (2004).

<sup>13</sup>H. D. Deng, J. Liu, W. R. Zhao, W. Zhang, X. S. Lin, T. Sun, Q. F. Dai, L. J. Wu, S. Lan, and A. V. Gopal, *Appl. Phys. Lett.* **92**, 233103 (2008).

<sup>14</sup>J. W. Seo, S. J. Park, and K. O. Jang, *J. Appl. Phys.* **85**, 5956 (1999).

<sup>15</sup>S. L. Pu, X. F. Chen, L. J. Chen, W. J. Liao, Y. P. Chen, and Y. X. Xia, *Appl. Phys. Lett.* **87**, 021901 (2005).

<sup>16</sup>H. E. Horng, C. Y. Hong, S. L. Lee, C. H. Ho, S. Y. Yang, and H. C. Yang, *J. Appl. Phys.* **88**, 5904 (2000).

<sup>17</sup>H. E. Horng, S. Y. Yang, S. L. Lee, C. Y. Hong, and H. C. Yang, *Appl. Phys. Lett.* **79**, 350 (2001).

<sup>18</sup>J. Monin, O. B. Philibert, V. Cabuil, and L. Delaunay, *Proc. SPIE* **1274**, 316 (1990).

<sup>19</sup>G. V. Kurllyandskaya, M. L. Sánchez, B. Hernando, V. M. Prida, P. Gorria, and M. Tejedor, *Appl. Phys. Lett.* **82**, 3053 (2003).

<sup>20</sup>A. T. Skjeltorp, *Phys. Rev. Lett.* **51**, 2306 (1983).

<sup>21</sup>R. Toussaint, J. Akselvoll, G. Helgesen, A. T. Skjeltorp, and E. G. Flekkøy, *Phys. Rev. E* **69**, 011407 (2004).

<sup>22</sup>A. T. Skjeltorp, *J. Appl. Phys.* **55**, 2587 (1984).

<sup>23</sup>R. M. Erb, H. S. Son, B. Samanta, V. M. Rotello, and B. B. Yellen, *Nature (London)* **457**, 999 (2009).

<sup>24</sup>A. Ashkin, *Biophys. J.* **61**, 569 (1992).

<sup>25</sup>W. H. Wright, G. J. Sonek, and M. W. Berm, *Appl. Phys. Lett.* **63**, 715 (1993).

<sup>26</sup>S. Y. Yang, Y. F. Chen, H. E. Horng, C. Y. Hong, W. S. Tse, and H. C. Yang, *Appl. Phys. Lett.* **81**, 4931 (2002).

<sup>27</sup>Y. T. Wu, X. G. Huang, and H. Su, *Appl. Phys. Lett.* **91**, 131101 (2007).

<sup>28</sup>B. Hoffmann and W. Köhler, *J. Magn. Magn. Mater.* **262**, 289 (2003).

<sup>29</sup>Q. F. Dai, H. D. Deng, W. R. Zhao, J. Liu, L. J. Wu, S. Lan, and A. V. Gopal, *Opt. Lett.* **35**, 97 (2010).

<sup>30</sup>Lord. J. W. S. Rayleigh, *Philos. Mag.* **32**, 529 (1916).

<sup>31</sup>Q. Li, Y. Xuan, and J. Wang, *Exp. Therm. Fluid Sci.* **30**, 109 (2005).